The anisotropic photorefractive effect in bulk As_2S_3 glass induced by polarized subgap laser light

1995 J. Phys.: Condens. Matter 7 1737

(http://iopscience.iop.org/0953-8984/7/8/020)

J. Phys.: Condens. Matter 7 (1995) 1737–1747. Printed in the UK

The anisotropic photorefractive effect in bulk As_2S_3 glass induced by polarized subgap laser light

V K Tikhomirov† and S R Elliott
Department of Chemistry, Cambridge University, Lensfield Road, Cambridge CB2 1EW, UK

Received 4 August 1994

Abstract. A strong, optically anisotropic, metastable photorefractive effect is observed in bulk As_2S_3 glass when illuminated with a subgap polarized He–Ne laser beam. When the laser beam is focused at or near the front surface of the sample, well resolved diffractive, optically anisotropic patterns appear in the transmitted beam in the course of irradiation; i.e. a novel kind of one-beam polarized self-induced holography can be recorded in this material. The microscopic mechanism of the observed effects is considered to consist of two components: a scalar (optically irreversible) component, due to the creation of randomly directed dipole moments, with a concentration $\sim 6 \times 10^{18}$ cm^{-3} and a vectoral (optically reversible) component, due to the reorientation of intrinsic (native) dipole moments, with a concentration $\sim 3 \times 10^{17}$ cm^{-3}, according to the electric vector of the inducing light.

1. Introduction

Chalcogenide semiconducting glasses are light sensitive media, i.e. many of their physicochemical properties can be changed in the course of irradiation [1–3]. It is surprising, however, that investigations of photoinduced effects in these materials have been carried out mainly on thin-film samples illuminated by strongly absorbed light (causing interband transitions).

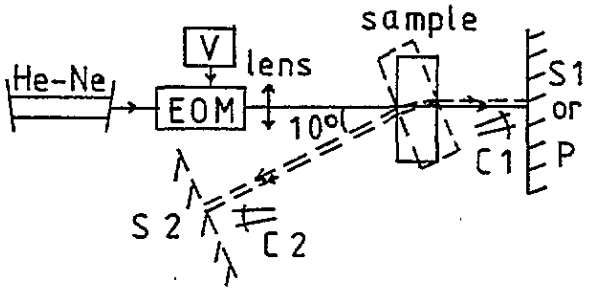

Figure 1. The optical set-up of the experiments.

Recently, investigations of photoinduced effects in bulk chalcogenide glasses have been undertaken [4, 5]. Subgap, polarized lasers were used as sources for the inducing light

† On leave from the A F Ioffe Physical–Technical Institute, St Petersburg, Russia.

0953-8984/95/081737+11$19.50

(absorption coefficient $\alpha \sim 1$–$10\ \mathrm{cm}^{-1}$) and several interesting effects were observed: in particular, very pronounced photoinduced anisotropy and diffuse light scattering. In these experiments, large focal lengths of lenses used to focus the laser beams, and unfavourable conditions of focusing, as well as diffuse light scattering in [4] (whose origin is discussed later), masked the interesting effects we report here.

When using a focused, polarized, subgap He–Ne laser beam, well resolved circular diffraction patterns (Fresnel zone-like or Newton ring-like) appeared in transmission on a screen placed behind the bulk glassy (g-) As_2S_3 sample and changed in appearance during irradiation. If, after some period of irradiation, the polarization of the light was switched to an orthogonal state, the pattern changed markedly.

It is suggested that the observed effects result from a novel kind of holography, i.e. one-beam, polarization dependent, self-induced bulk holography. The microscopic mechanism of the observed effects is suggested to be due to a combination of two mechanisms: a scalar (optically irreversible) component, associated with the creation of randomly directed dipole moments, with concentration $\sim 6 \times 10^{18}\ \mathrm{cm}^{-3}$ and a vectoral component (optically reversible), associated with the reorientation of intrinsic (native) dipole moments with a concentration $\sim 3 \times 10^{17}$ according to the electric vector of the inducing light. These results offer the prospect of new applications of bulk chalcogenide glasses.

2. Experimental details

The bulk As_2S_3 glasses studied were of good optical quality and transparent in the infrared (i.e. they have a very low level of impurities). The samples were cut and have at least two parallel polished faces; the distance between the faces ranges between 1 mm and 10 mm.

The optical set-up of the experiments is shown in figure 1. The beam of an He–Ne laser ($P \sim 1$ mW, $h\nu = 1.96$ eV) passed through an electro-optical modulator (EOM), controlled by an electrical DC or AC voltage (V), which can change the polarization of the beam between two mutually orthogonal states either for long periods or with a frequency $\sim$1 kHz. The optical gap of glassy As_2S_3 is 2.3 eV, i.e. much higher than the quantum energy of the laser light. The absorption coefficient (or more strictly speaking, the extinction coefficient) of As_2S_3 for $h\nu = 1.96$ eV is about $1.0\ \mathrm{cm}^{-1}$. The beam was focused with a short-focal-length lens ($f \sim 2.5$ cm) either on the front surface of the sample or on the back surface of the sample. The laser beam was arranged to be at approximately normal incidence on the sample (solid lines in figure 1) as well as at an inclined angle of incidence (dashed lines in figure 1). In the former case, we registered only the transmitted light beam by means of screen 1 (S1) and camera 1 (C1) or by means of a photodetector (P); in the latter case, we registered both transmitted and reflected beams by means of screen 1 and camera 1 and screen 2 (S2) and camera 2 (C2), respectively. The cameras were positioned at small angles to the normal to the screens.

The entrance window of the photodetector has a diameter of 1 cm. The signal from the photodetector was measured with a lock in amplifier and/or oscilloscope using the method described in [4].

3. Results

Figures 2 and 3 show characteristic photographs to illustrate the qualitatively important aspects of the data. Only data obtained using an inclined beam focused at, or just before, the front surface of the sample are presented. More details will be given elsewhere.

Figure 2(a)–(c) shows pictures taken with camera 1. Here the polarization of light was held constant throughout, and we refer to this case as $E_\parallel$. The incident beam intensity was kept constant. At the beginning of the irradiation, the spot of the transmitted beam observed on screen 1 (figure 2(a)) was intense (although very weak rings were also observed around the central spot, probably due to some transient effect). A dramatic change of the transmitted beam was observed in the course of the irradiation, as illustrated by figure 2(b), (c).

Three systems of rings (marked as A, B, C) are evident in figure 2(c). The system of very narrow, rather incomplete, rings (marked A) with small spacings near the centre might be the result of light scattered from dust on the sample surface, from imperfections in the sample itself or from a self-focused lens [6].

At larger radii, another system (marked as B) of thin rings is observed, with larger separations, apparently somewhat similar to Newton's rings/Fresnel zones. The diameters of these rings approximately satisfy the relation characteristic of Newton's ring/Fresnel zone formation, viz. $R_m \sim \sqrt{m}$, where R_m is the radius of dark rings and m is an integer. If we assume that $R_m = (m\lambda\rho)^{1/2}$, where ρ is the radius of curvature of the Newton lens (in the present case, assumed to be formed within the sample by a photoinduced refractive index change in the course of illumination), and λ is the wavelength of the light, then we obtain $\rho \sim 400$ m, which is unphysical. Moreover, the conditions necessary to give rise to Newton's rings, i.e. multibeam interference, do not apply in the present case due to the inclined angle of incidence of the incident beam. In addition, interference inside the thick sample studied is precluded due to the high extinction of light and the inclined angle of the incident beam, leading to a separation of the beams inside the sample that could interfere, as seen from the separation of images in figure 3.

A similar square root dependence, $R_m = (2m\lambda D)^{1/2}$ (where D is the distance between sample and screen), is also expected from the collinear illumination and scattering from a point object giving rise to simple Gabor holography [7]. From this relation, the separation between neighbouring rings is $R_{m+1} - R_m = (\lambda D)/(2R_m) \approx 10$ μm, in contrast to the experimentally observed value ~ 1 mm. Taking into account that our source is not collinear, but is a laser beam focused by a lens with focal length ~ 25 mm, that refraction of light takes place at the back face of the sample and the sample–screen separation is ~ 1 m, a magnification factor of 100 may exist, leading to consistency between calculated and observed values.

Finally, there appears to be an intensity modulation (like dark and bright haloes, marked as C) superimposed on the set of Fresnel zones in figure 2(c), somewhat similar to that expected from diffraction by a circular extended obstacle.

Figure 2(d) shows the diffraction patterns when switching the polarization of the incident beam to an orthogonal state (referred to here as $E_\perp$) for a short period (~ 1 s) after 20 min of irradiation by a beam with electric vector $E_\parallel$. (We emphasize that no changes of the transmitted beam are observed for such short periods, i.e. the beam with $E_\perp$ polarization can be considered as a probe.) A difference between the patterns in figure 2(c) and (d) is clearly seen, indicating the existence of optical anisotropy of the diffractive object photoinduced in the sample. (No differences between the transmitted beams with $E_\parallel$ and $E_\perp$ were observed just at the beginning of the irradiation, indicating that the sample was isotropic before irradiation.)

Figure 3(a), (b) shows pictures taken with camera 2 for (a) $E_\parallel$ and (b) $E_\perp$ polarizations of the incident beam. Note two features, as follows. (i) Images of beams reflected from the front and back faces are very different; the former is the same as an Airy disc, the latter is strictly the same as the image of the transmitted beam observed on screen 1 (figure 2(c) and

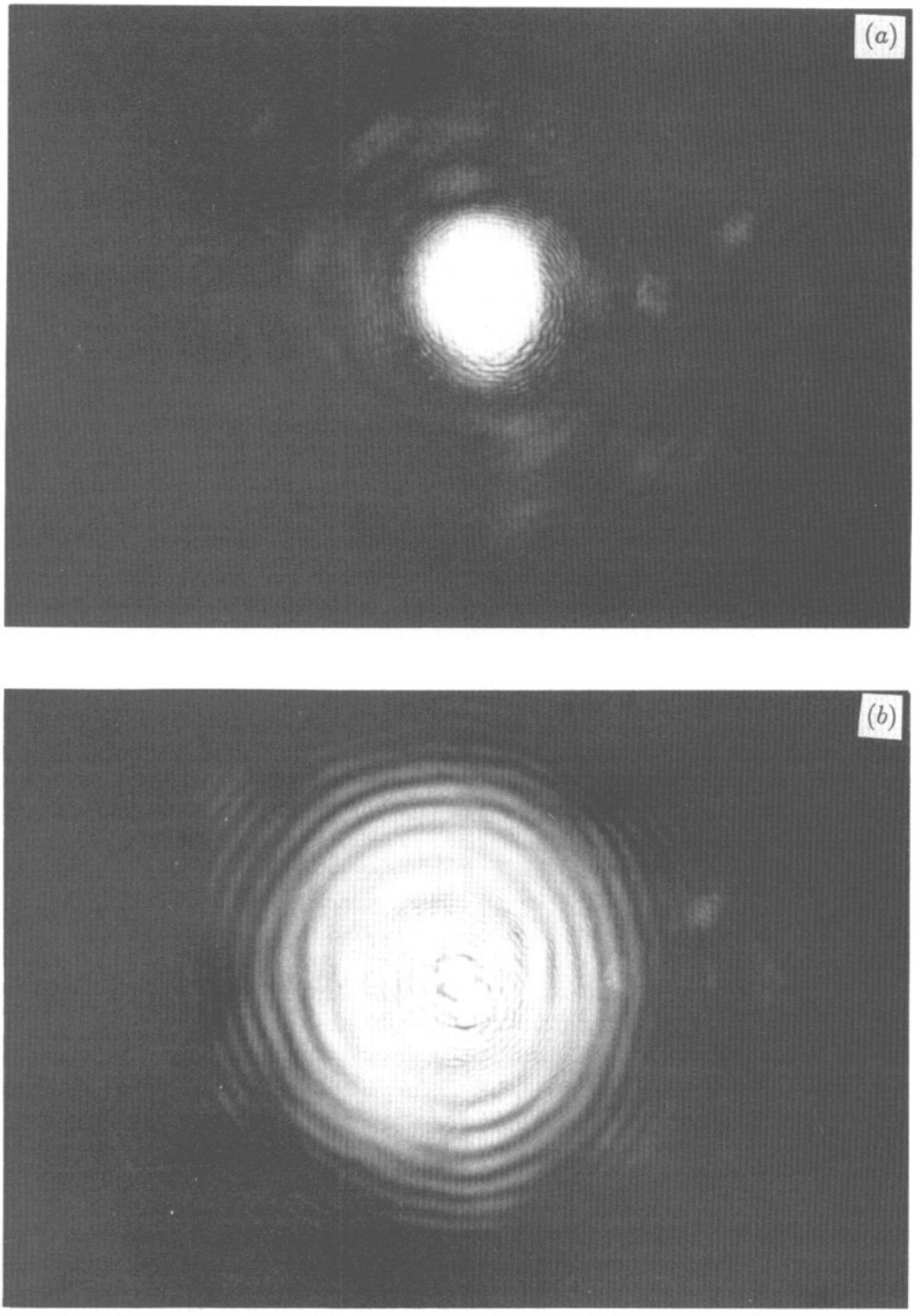

Figure 2. Characteristic photographs taken with camera 1 right at the beginning (a) and after 10 min (b) and 20 min (c), (d) of irradiation by an He–Ne laser beam with intensity ~ 1 mW and constant polarization (a)–(c) or when switching the polarization to the orthogonal state for a short period (d). The sample was a 5 mm thick piece of As_2S_3 glass. Screen 1 is 1 m from the sample.

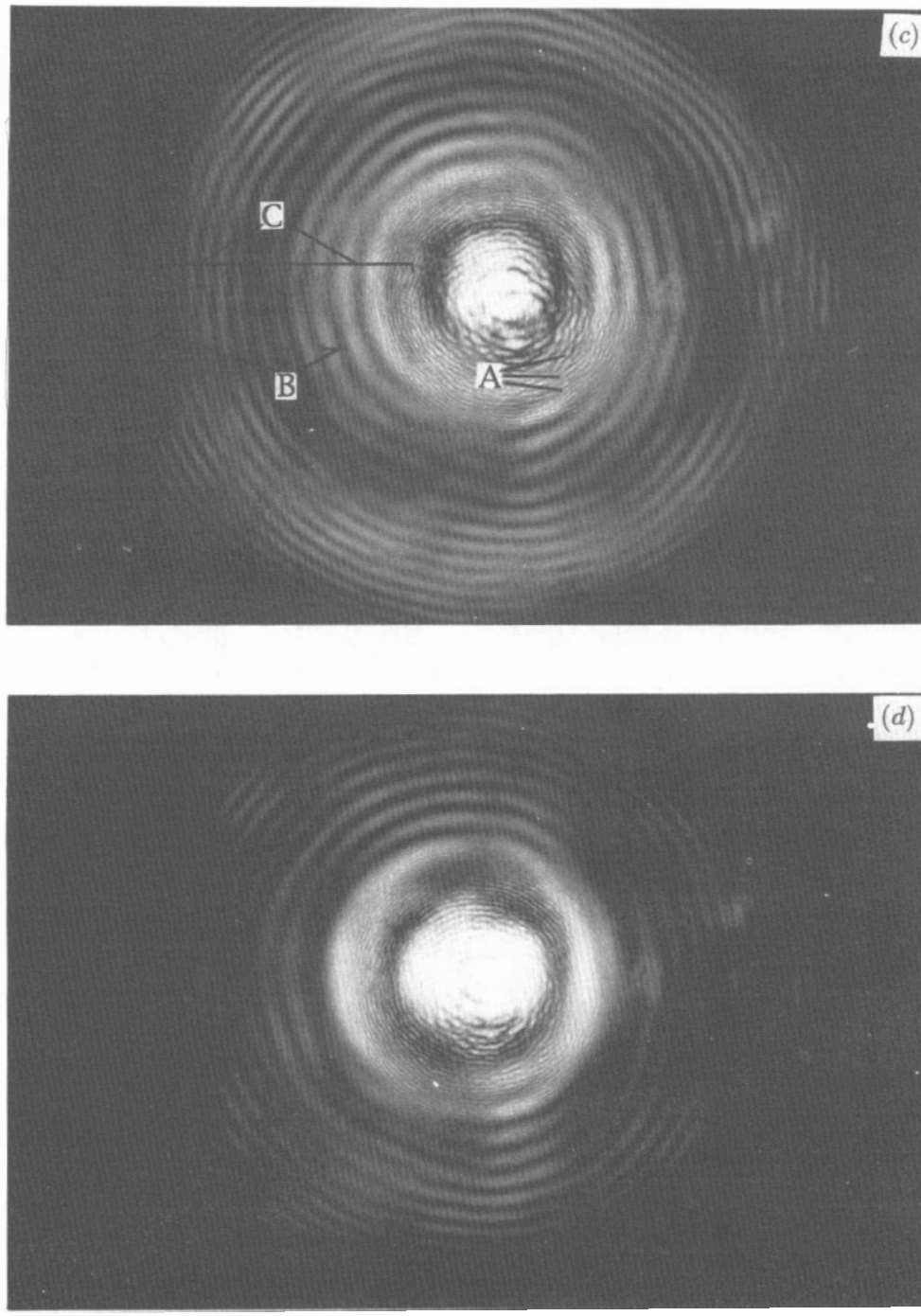

Figure 2. (Continued)

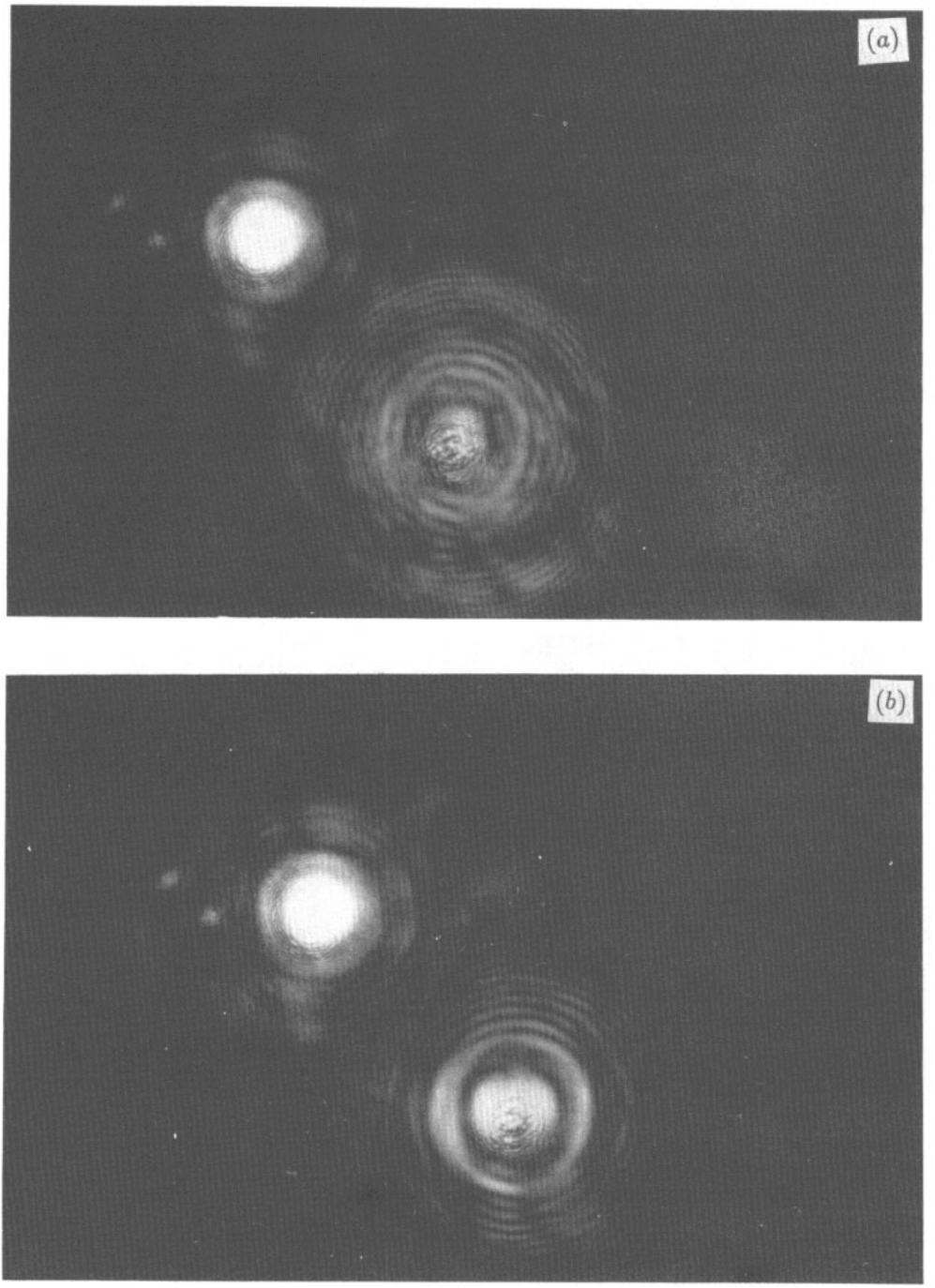

Figure 3. Characteristic photographs (a), (b) taken with camera 2 in the same conditions as in figure 2(c), (d) respectively. The left-hand and right-hand images correspond to beams reflected from the front and back faces of the sample respectively. Screen 2 is 0.5 m from the sample.

(d)). Thus the object that diffracts the beam is formed *inside* the sample and no multiple-beam interference takes place. (ii) No anisotropy is observed for beams with $E_\parallel$ and $E_\perp$ reflected from the front face, i.e. the anisotropic change also occurs inside the sample.

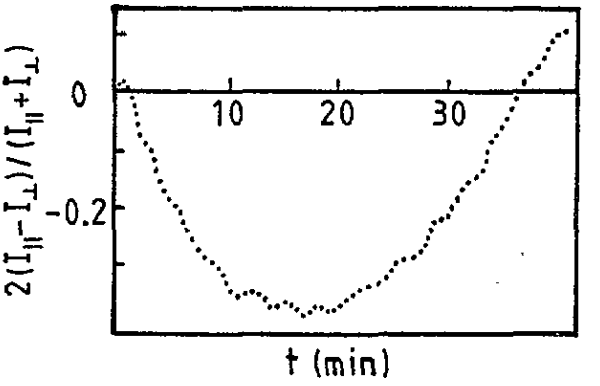

Figure 4. Kinetics of transmittance anisotropy $2(I_\parallel - I_\perp)/(I_\parallel + I_\perp)$ registered with a photodetector in the central part of the image of the diffraction pattern.

Typical kinetics of the transmittance anisotropy $2(I_\parallel - I_\perp)/(I_\parallel + I_\perp)$ registered with a photodetector as in [4] are shown in figure 4. Here $I_\parallel$, $I_\perp$ are the intensities of beams with polarizations $E_\parallel$, $E_\perp$ transmitted through the sample and accepted by the entrance window of the photodetector, respectively. The quantities $I_\parallel - I_\perp$ and $(I_\parallel + I_\perp)/2$ were measured by means of a lock in amplifier and an oscilloscope, respectively, whilst modulating the polarization direction of the probe light between $E_\parallel$ and $E_\perp$ with a frequency of 1 kHz. Two features are apparent: (i) large-amplitude, long-period oscillations and (ii) small-amplitude, short-period oscillations. The former oscillations correspond to the appearance and changes in the diameter and in the intensity of the broad haloes (C) and the latter correspond to changes in the diameter of the Fresnel zones (B). The signal $2(I_\parallel - I_\perp)/(I_\parallel + I_\perp)$ is due to the fact that the diameters and intensities of the rings and haloes are different for the polarizations $E_\parallel$ and $E_\perp$, leading to differences in $I_\parallel$ and $I_\perp$. This signal may be affected also by photoinduced dichroism accompanying photoinduced birefringence.

In conclusion, we add that a memory effect takes place; i.e. when the incident beam is switched off for a couple of days, and then switched on again, the well resolved diffractive patterns appear again just after switching on the laser beam. A partial relaxation of the photoinduced anisotropy takes place when the sample is stored in the dark. Detailed studies of the dark relaxation, as well as the response of the optical anisotropy to multiple switching off and on of the light, appear elsewhere [8, 9].

4. Discussion

We suggest an explanation for the data reported in this paper based on the principle of Gabor holography, which uses a source and an obstacle arranged collinearly [10]. There are several principal differences to the normal Gabor holography situation in our case.

(i) Instead of a point source, we use the caustic of a focused laser beam.

(ii) Instead of an obstacle, a three-dimensional diffractive object exists (most probably lens shaped initially, and cone shaped due to self-focusing in the final stages of irradiation),

which is photoinduced in the bulk of the chalcogenide glass after prolonged irradiation by subgap light. Certainly, the form of this object, most probably located at the apex of this cone, is determined by the irradiation conditions (e.g. focal length of lens, relative distance between sample and caustic of the laser beam, intensity distribution in the cross section of the laser beam etc); i.e. the object can, in principle, be created in any desirable form. This is supported by our observation that the character of the patterns is very strongly changed when the laser beam is focused on the back face of the sample. The origin of this object, obviously, is due to a photoinduced metastable change of the refractive index (photorefraction) inside the region where the laser beam propagates. Certainly, additional self-focusing of the laser beam inside the sample takes place due to the non-uniform (Gaussian) distribution of intensity in the cross-section of the laser beam and a corresponding non-uniform photorefractive effect inside the sample, i.e. the object is self-induced.

Self-focusing of laser beams and accompanying diffractive effects have been discussed in the literature, e.g. [11]. However, three new points arise in our case: (i) the change of refractive index is anisotropic; (ii) the light intensity required is several orders of magnitude lower compared to previous cases [11]; (iii) the photoinduced object is optically anisotropic, i.e. photoinduced, metastable birefringence takes place. The optical axis of the object can be reoriented many times according to the electric vector of the inducing incident beam.

The small-amplitude oscillations in figure 4 are due to a change in the diameters of the thin rings (B) in figure 2 (which are different for $E_\parallel$ and $E_\perp$ polarizations) during the course of irradiation. One period of these oscillations corresponds to the movement of one zone of the Fresnel pattern relative to the entrance window of the photodetector. That is,

$$\delta = 2\pi \Delta n\, h/\lambda = 2\pi \tag{1}$$

where δ and Δn are respectively the phase difference and change of the refractive index corresponding to the movement of one zone of the Fresnel pattern relative to the entrance window of the photodetector, and h is the thickness of the sample where the change of n takes place. From (1) $\Delta n = \lambda/h \sim 1.2 \times 10^{-4}$. (We assume that h is constant, because the photoinduced changes mostly occur inside the sample, as seen from figures 2 and 3.) This value, multiplied by the number of oscillations in figure 4, gives the degree of photorefraction reached at the end of the experiment in figure 4, which is about 1.8×10^{-3}.

The birefringence can be estimated from the shift of the pattern when switching the light polarization to the orthogonal state. This shift is visually detectable in our case and corresponds to about one ring; that is, the birefringence, corresponding to figure 4, is about $n_\parallel - n_\perp \simeq 1.2 \times 10^{-4}$. This value is two orders of magnitude higher than the photoinduced birefringence in Ge doped silica fibres [12]; i.e. this is interesting for applications. The origin of the sign of the birefringence is discussed elsewhere [13, 14].

The mechanism we propose to explain the observed anisotropic photorefractive effect consists of two processes: scalar and vectoral. The photoinduced creation of metastable microscopic electric dipoles in the glass is a scalar effect. Since no special impurities exist in chalcogenide glasses (such as for example Ge impurities in germanosilicate glasses [12, 15] or Fe^{2+}, Fe^{3+} impurities in $BaTiO_3$ crystals [16], which are known as photorefractive materials), we suggest that two specific kinds of 'native defect' exist in glassy chalcogenides. Excitation of the first kind of defect (normally electrically neutral) leads to the formation of electric dipoles in glass. We suggest that these defects are wrong bonds, e.g. As–As [17]. The breakage of such As–As wrong bonds [1–3, 17] yields positively charged As^+ centres and trapped electrons. In support of the involvement of As–As bonds, investigations of the photorefractive effect in glassy As_xS_{1-x}, with varying x, show that the photorefraction

effect strongly decreases with decreasing x [18]. Furthermore, photorefraction (as well as the accompanying effect of photodarkening) is rather weak in or even absent from chalcogenide glasses that do not contain As (e.g. Se, Sb_2S_3, Ge_2PbS_3), where the vectoral effects of photoinduced birefringence and accompanying dichroism still exist and are even much more pronounced (e.g. in Sb_2S_3 and Ge_2PbS_3) compared to As containing glasses [19].

Each resulting 'photoinduced' dipole produces a microscopic frozen in polarization field, which gives a local change of refraction $\Delta n \sim \chi^{(3)} E_{\mathrm{dip}}^2$, where E_{dip} is the electric field of the dipole and $\chi^{(3)}$ is the cubic term of the susceptibility. Assuming, following [15], that the total energy stored in this dipole field is comparable with the energy of an absorbed quantum of light and that $\Delta n = f(\chi^{(3)}, N_{\mathrm{n}})$, where N_{n} is the number density of dipoles, we obtain (after [15])

$$N_{\mathrm{n}} = \left(\Delta n \sqrt{n_0} \varepsilon_0 \varepsilon_r\right) / \left(3\chi^{(3)} h\nu\right) = 6 \times 10^{18}\ \mathrm{cm}^{-3} \tag{2}$$

where $\Delta n = 1.8 \times 10^{-3}$, $n_0 = 2.5$ and $\varepsilon_{\mathrm{r}} = 8$ [20]. Note that the value of $\chi^{(3)}$ used is 6×10^{-12} esu $= 8.3 \times 10^{-20}$ $\mathrm{m}^2\ \mathrm{V}^{-2}$ [21], i.e. two or three orders of magnitude higher than in silica glasses [15]. This is the main reason why such a small concentration N_{n} of dipoles leads to such a pronounced macroscopic effect Δn.

We stress that this mechanism can cause only a scalar change of refraction, because the positions of traps are randomly situated relative to As^+ sites in the glass and have no correlations with the electric vector of the inducing light. We consider this mechanism to be a photorefractive effect because it is based on charge generation and separation followed by trapping of carriers and creation of self-trapped exciton defects. We believe that impurities do not play a significant role in producing the observed effects since the same behaviour is found in samples prepared by different methods in different laboratories where it might be expected that the level of impurity content might vary appreciably.

We suggest a second process, responsible for the vectoral birefringence effect, is the orientation of pre-existing defects of another kind. These are valence alternation pairs D^+D^- [22] or $C_3^+C_1^-$ [23], where D or C is a chalcogen. These are sensitive to the polarization state of light and can be reoriented many times in accordance with the electric vector of the inducing light [4, 14, 18, 19].

From our data, the photoinduced birefringence $n_\parallel - n_\perp = 1.2 \times 10^{-4}$ after prolonged illumination is about an order of magnitude smaller than the scalar photorefraction at the same time. We assume that, in contrast to the case considered above, the energy of the absorbed photons is used, not to create new dipoles, but rather for the orientation of the intrinsic dipoles. In this case, the relation

$$N_{\mathrm{ch}} = \left((n_\parallel - n_\perp)\sqrt{n_0} \varepsilon_0 \varepsilon_{\mathrm{r}}\right) / \left(3\chi^{(3)} h\nu\right) = 3 \times 10^{17}\ \mathrm{cm}^{-3} \tag{3}$$

is valid, where $n_\parallel - n_\perp$ is the birefringence caused by orientation of D^+D^- ($C_3^+C_1^-$) dipoles. The origin of the negative effective correlation energy leading to valence alternation pairs is based on the specific ability of chalcogen atoms to have different coordinations. This feature does not depend on the As content. Previous studies [18] showed a very weak dependence of $n_\parallel - n_\perp$ on x in the glassy system As_xS_{1-x}. In addition, an increase of the vectoral effect, in contrast to a decrease of the scalar effect, is observed in chalcogenide glasses that do not contain As atoms (e.g. Sb_2S_3 and Ge_2PbS_3) [19], compared to As_2S_3, supporting the notion of a difference in the origin of N_{n} and N_{ch} defects. Note that previous estimates

[24, 25] for the concentration of valence alternation pairs give approximately the same value as from (3). It is seen from these considerations that neither scalar nor vectoral effects can be explained simply by thermo-optic (heating) effects. A more detailed microscopic model for the vectoral effect is given in [8].

Finally, we note that, in some special cases, the well resolved patterns of figure 2 are replaced by diffuse light scattering with a speckle structure, as in [4]. (This is often observed in As_2S_3 alloyed with I.) We have observed that the speckle structure is observed only in the transmitted beam, but not in the reflected beam, where the Airy disc or well resolved patterns are always observed. This can be explained as a result of interference due to diffuse scattering of the laser beam from imperfections in the sample, which, in addition, can be amplified inside the sample due to non-linear beam coupling, as in [16]. We have found that the speckle structure can be avoided in the case of the chalcogenide glass $As_2S_3I_{0.8}$ by means of annealing or thorough polishing of the front face (to eliminate roughness, or products of oxidation or crystallization on the front surface). The noise of the laser beam can also play an important role in the appearance of diffuse light scattering.

5. Conclusion

After irradiating a semiconducting chalcogenide bulk glass (As_2S_3) with the linearly polarized subgap light beam of an He–Ne laser focused on the front surface of the sample, well pronounced optically anisotropic patterns (Fresnel zones) appeared and changed during the course of irradiation, as monitored in transmission by a screen placed behind the sample. This effect is considered to result from a novel kind of one-beam, polarization dependent, self-induced holography based on an anisotropic photorefractive effect taking place inside the bulk of the sample and accompanying diffractive phenomena. The microscopic mechanism of the observed effects is supposed to comprise two parts: photoinduced creation of randomly oriented dipole moments with a concentration 6×10^{18} cm^{-3}, which is not dependent on the polarization of the inducing light (scalar effect), and photoinduced reorientation of pre-existing native dipoles (valence alternation pairs) with a concentration 3×10^{17} cm^{-3}, in accordance with the electric vector of the inducing light (vectoral effect). These results offer the prospect of new applications of bulk chalcogenide glasses.

Acknowledgment

V K Tikhomirov should like to acknowledge the Royal Society for providing him with a post-doctoral fellowship. The authors thank Professor Keiji Tanaka of Hokkaido University for bringing to their attention [16]. The high-purity As_2S_3 glasses studied here were prepared in the laboratories of S A Dembovskii and Z U Borisova.

References

[1] Elliott S R 1986 *J. Non-Cryst. Solids* **81** 71
[2] Tanaka K 1990 *Rev. Solid State Sci.* 4 641
[3] Pfeiffer G, Paesler M A and Agarwal S C 1991 *J. Non-Cryst. Solids* **130** 111
[4] Lyubin V M and Tikhomirov V K 1991 *J. Non-Cryst. Solids* **135** 37; 1991 *J. Non-Cryst. Solids* **137&138** 993
[5] Shiramine K, Hisakuni H and Tanaka K 1994 *Appl. Phys. Lett.* **64** 1771

Hisakuni H and Tanaka K 1994 *Solid State Commun.* **90** 483
[6] Born M and Wolf E *Principles of Optics* (Oxford: Pergamon) p 456
[7] Françon M 1979 *Optical Image Formation and Processing* (New York: Academic) pp 42, 100
[8] Tikhomirov V K and Elliott S R 1995 *Phys. Rev.* B at press
[9] Tikhomirov V K 1993 *JETP Lett.* **57** 821
[10] Stroke G W 1969 *An Introduction to Coherent Optics and Holography* (New York: Academic)
[11] Chiao R Y, Garmire E and Townes C H 1964 *Phys. Rev. Lett.* **13** 479
[12] Ouellette F, Gagnon D and Poirier M 1991 *Appl. Phys. Lett.* **58** 1813
[13] Tikhomirov V K and Elliott S R 1994 *Phys. Rev.* B **49** 17476
[14] Fritzsche H 1994 *J. Non-Cryst. Solids* **164–166** 1169
[15] Hand D P and Russell P St J 1990 *Opt. Lett.* **15** 102
[16] Segev M, Engin D, Yariv A and Valley G 1993 *Opt. Lett.* **18** 956
[17] Elliott S R 1991 *Materials Science and Technology—A Comprehensive Treatise* vol 9, ed J Zarzycki (VCH) p 375
[18] Lyubin V M and Tikhomirov V K 1991 *Sov. Phys.–Solid State* **33** 1161
[19] Lyubin V M and Tikhomirov V K 1991 *J. Non-Cryst. Solids* **114** 133; 1990 *Sov. Phys.–Solid State* **32** 1069
[20] Borisova Z U 1981 *Glassy Semiconductors* (New York: Plenum) p 135
[21] Asobe M, Suzuki K, Kanamori T and Kubodera K 1992 *Appl. Phys. Lett.* **60** 1153
[22] Mott N F, Davis E A and Street R A 1975 *Phil. Mag.* B **32** 961
[23] Kastner M, Adler D and Fritzsche H 1976 *Phys. Rev. Lett.* **37** 1504
[24] Kastner M and Fritzsche H 1978 *Phil. Mag.* B **37** 199
[25] Vanderbilt D and Joannopoulos J D 1981 *Phys. Rev.* B **23** 2596